Solid-State Electronics 194 (2022) 108335

Contents lists available at ScienceDirect

Solid State Electronics

journal homepage: www.elsevier.com/locate/sse

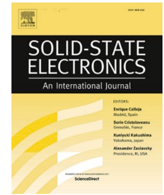

Double Reference Layer STT-MRAM Structures with Improved Performance

Wilton Jaciel Loch [a,*], Simone Fiorentini [a,b], Nils Petter Jørstad [a], Wolfgang Goes [c], Siegfried Selberherr [b], Viktor Sverdlov [a,b]

[a] Christian Doppler Laboratory for Nonvolatile Magnetoresistive Memory and Logic at the Institute for Microelectronics, TU Wien, Gußhausstraße 27-29, A-1040 Wien, Austria
[b] Institute for Microelectronics, TU Wien, Gußhausstraße 27-29, A-1040 Wien, Austria
[c] Silvaco Europe Ltd., Cambridge, United Kingdom

ARTICLE INFO

Keywords:
MRAM
Finite element method
Spin-transfer torque
Magnetic tunnel junction
Magnetic switching

ABSTRACT

MRAM structures employing two ferromagnetic layers with fixed magnetization were recently introduced in experimental works, allowing the reduction of both switching currents and cell sizes. We verify by means of simulation their improved switching characteristics over structures with a single fixed magnetization layer.

1. Introduction

Spin-transfer torque magnetoresistive random-access memory (STT-MRAM) is an emerging technology set to potentially replace conventional flash memory, DRAM, and slow SRAM, due to its nonvolatility and increasingly improved power consumption, high storage density, fast writing speed, strong endurance, and long data retention. As shown in Fig. 1a, STT-MRAM devices are composed of a ferromagnetic (FM) reference layer (RL), with fixed magnetization orientation, an insulator tunnel barrier (TB), and a ferromagnetic free layer (FL), with variable magnetization orientation. The conjunction of these three layers forms a magnetic tunnel junction (MTJ) and since this is the central component of the cell, the whole structure is hereafter referred to as single MTJ (SMTJ). Information is stored based on different resistance levels which appear, when the FL magnetization is set to either parallel (P) or anti-parallel (AP) to the RL magnetization orientation. Changes between these magnetization states are achieved by passing sufficiently large currents through the structure parallel to the layer stack [1].

Currently, one of the challenges faced by STT-MRAM devices is their miniaturization to achieve increased storage densities, which would allow their use for a broader range of applications, expanding their competitiveness against regular volatile memories. The main path towards this goal is the reduction of the bit cell size which is primarily determined by the contact dimensions necessary to provide the switching currents. Thus, reducing the current, and likewise voltage, required to alternate between the two stable magnetization states also grants a transitively proportional reduction in the cell size.

Recently published works proposed structures with additional layers aiming at a reduction of the switching current and consequently the cell size. The most promising structure is the double spin-torque magnetic tunnel junction (DS-MTJ), which adds a non-magnetic (NM) spacer (SP) and a reference layer on top of the three conventional ones [2], as shown in Fig. 1b. The orientation of the second RL magnetization can be set to either parallel or anti-parallel to the original RL magnetization with the help of an external field. For simplicity, these two configurations are henceforth referred to as DS-MTJ$_P$ and DS-MTJ$_{AP}$, respectively. According to experimental data [2], the magnetization state of this additional RL will determine whether the FL switching will be shorter than the SMTJ, when anti-parallel to the first RL or longer, when parallel to the first RL.

Accurate simulations of the switching processes in such devices are of paramount importance to understand the interplay of involved parameters and their impact on the performance. To this end, the magnetization dynamics in STT-MRAM devices can be obtained by solving the extended Landau-Lifshitz-Gilbert (LLG) equation

$$\frac{\partial \mathbf{m}}{\partial t} = -\gamma\mu_0 \mathbf{m} \times \mathbf{H_{eff}} + \alpha \mathbf{m} \times \frac{\partial \mathbf{m}}{\partial t} + \frac{1}{M_S}\mathbf{T_S}, \quad (1)$$

where γ is the gyromagnetic ratio, μ_0 the vacuum permeability, $\mathbf{H_{eff}}$ the effective magnetic field, α the Gilbert damping constant and M_s the

* Corresponding author.
E-mail address: loch@iue.tuwien.ac.at (W.J. Loch).

https://doi.org/10.1016/j.sse.2022.108335
Received 29 March 2022; Received in revised form 18 April 2022; Accepted 19 April 2022
Available online 2 May 2022
0038-1101/© 2022 Elsevier Ltd. All rights reserved.

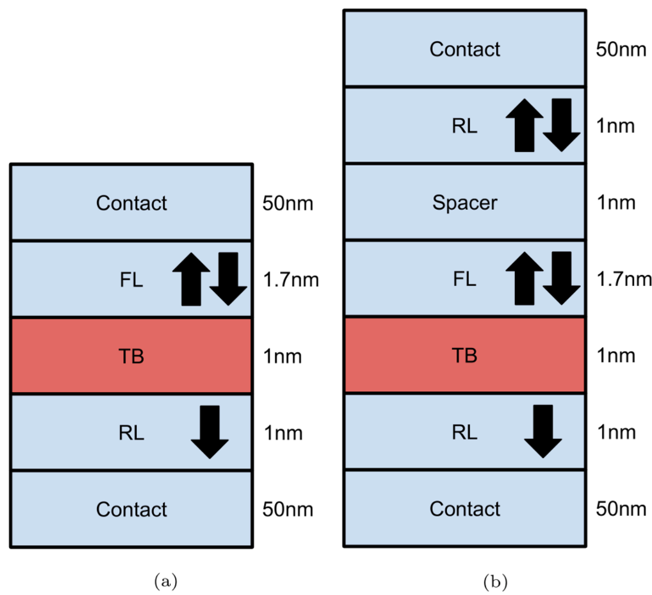

Fig. 1. Schematics of MTJ structures: (a) Three-layer SMTJ. (b) DS-MTJ with five layers.

Table 1
Material [2] and simulation [1,3] parameters.

Parameter	Value
Damping constant (α)	0.02
Saturation magnetization (M_s)	$1.2{\cdot}10^6$A/m
Exchange constant (A)	$1{\cdot}10^{-11}$J/m
Anisotropy constant (K)	$9{\cdot}10^5$J/m^3
Conductivity FM (σ_{FM})	$1{\cdot}10^6$A/(V · m)
Conductivity NM (σ_{NM})	$6{\cdot}10^6$A/(V · m)
Conductivity spin polarization (β_σ)	0.7
Diffusivity spin polarization (β_D)	0.8
Diffusion coefficient FM ($D_{e,FM}$)	$2{\cdot}10^{-3}$m^2/s
Diffusion coefficient NM ($D_{e,NM}$)	$1{\cdot}10^{-2}$m^2/s
Spin-flip length (λ_{sf})	10 nm
Spin dephasing length (λ_ϕ)	0.4 nm
Exchange length (λ_J)	1 nm
Resistance parallel (R_P)	4.3423 kΩ
Resistance anti-parallel (R_{AP})	9.0630 kΩ
Tunneling magnetoresistance	109%

saturation magnetization. The normalized magnetization $\mathbf{m}$ is given by $\mathbf{M}/M_s$ while $\mathbf{T}_\mathbf{S}$ represents the spin-torque due to polarized spin currents. We have previously developed a Finite Element-based simulator which enables the precise analysis of various structures and phenomena related to STT-MRAM devices. By solving the extended LLG while employing a coupled spin and charge transport approach for the torque calculation, this tool is able to evaluate the time-dependent magnetization of multi-layered structures composed of ferromagnets, metal spacers and tunnel barriers [3]. Therefore, we have employed the simulator to investigate the switching characteristics of the DS-MTJ and compared it with the SMTJ.

2. Simulation and Results

Each structure is modeled as a 40nm wide cylinder, with layer thicknesses and magnetizations defined as indicated in Fig. 1. The x-axis is employed as the anisotropy easy-axis. Resistances for each state were extracted from [2] and are presented in Table 1 alongside additional material parameters. The spacer is modeled as a non-magnetic conductor with the same parameters as the contacts.

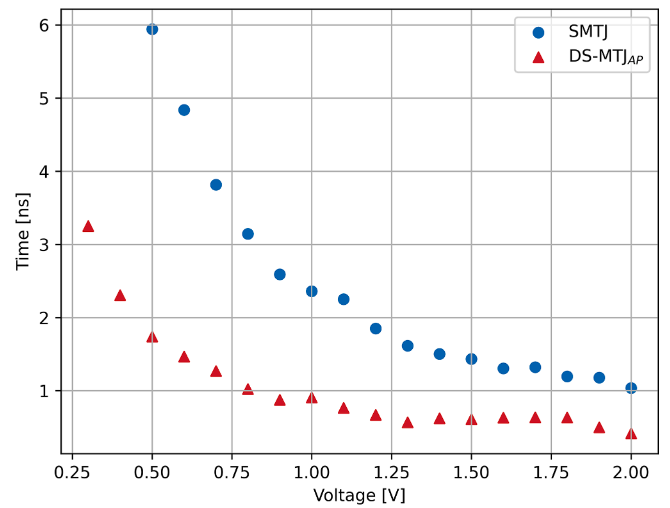

Fig. 2. Time required for the free layer magnetization to switch from parallel to anti-parallel with different applied voltages.

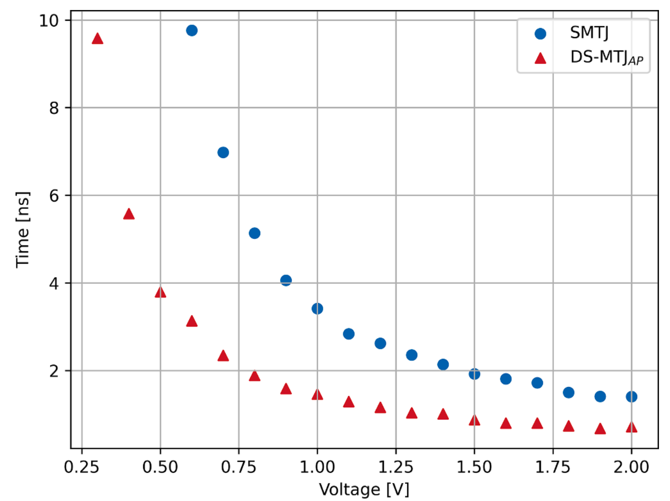

Fig. 3. Time required for the free layer magnetization to switch from anti-parallel to parallel with different applied voltages.

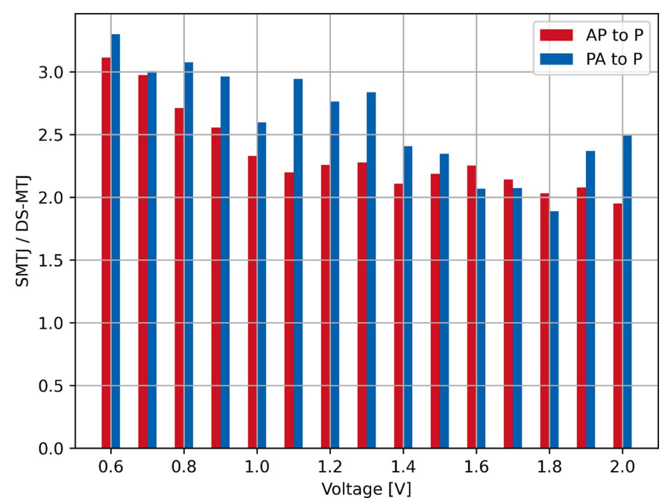

Fig. 4. Ratio between SMTJ and DS-MTJ$_{AP}$ switching times with different applied voltages.

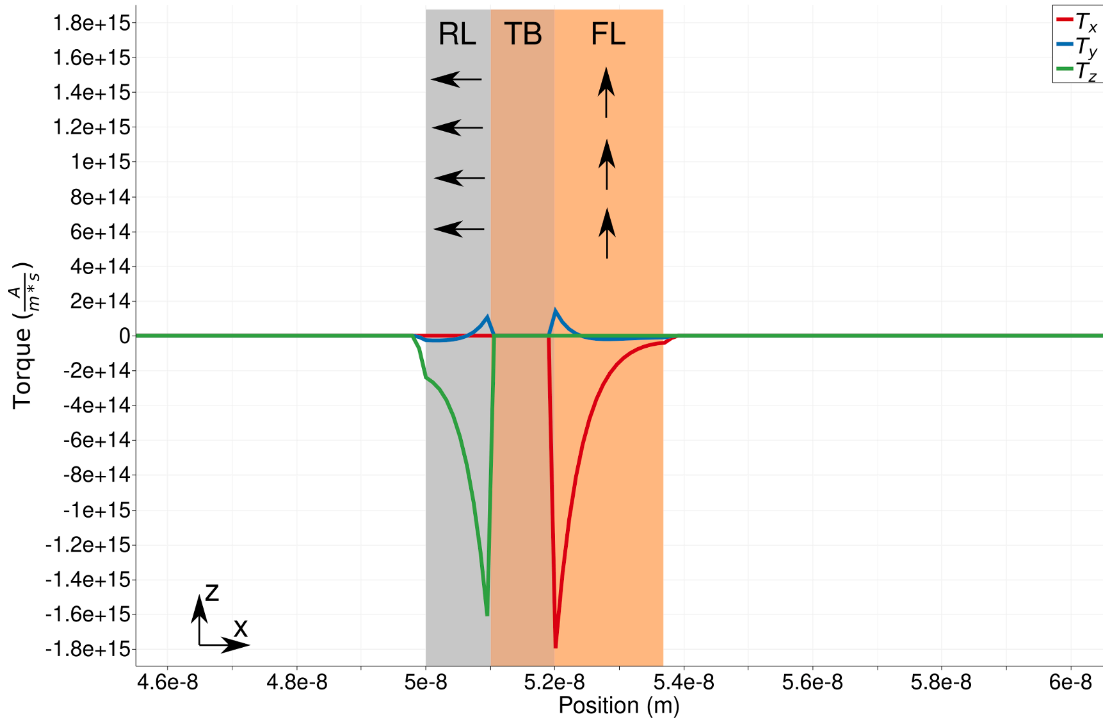

Fig. 5. Average torque on the SMTJ structure along the x-axis. The FL magnetization points in the $\hat{z}$ direction and RL points in $-\hat{x}$.

2.1. Switching times

Figs. 2 and 3 respectively show for both structures the required time for the FL magnetization to switch from parallel to anti-parallel and vice versa with 10ns write pulses. The magnetization is considered switched, when its normalized easy-axis component reaches 0.8 magnitude in the target direction. Simulations that failed to reach the target for each configuration were removed from the plot. In the two switching directions, when the same voltage is applied, the switching time of the DS-MTJ$_{AP}$ is consistently smaller than the time of the SMTJ. The latter has also not achieved the switching target in some of the lowest voltages on both plots. This indicates, as expected from experimental observations, that its threshold switching voltage is larger than that of the DS-MTJ$_{AP}$ for the two directions.

Fig. 4 summarizes the ratios between SMTJ and DS-MTJ$_{AP}$ observed switching times (when applicable). The tendency of the ratios to reduce as the voltage grows is related to the fact that as the DS-MTJ has a smaller switching voltage, it approaches a saturation regime earlier than the SMTJ, where the same addition in voltage translates to smaller switching time reductions. In this regime, although absolute differences are smaller, the DS-MTJ still maintains a close to 2 times reduction of the switching time. Overall, the average improvement achieved by the novel

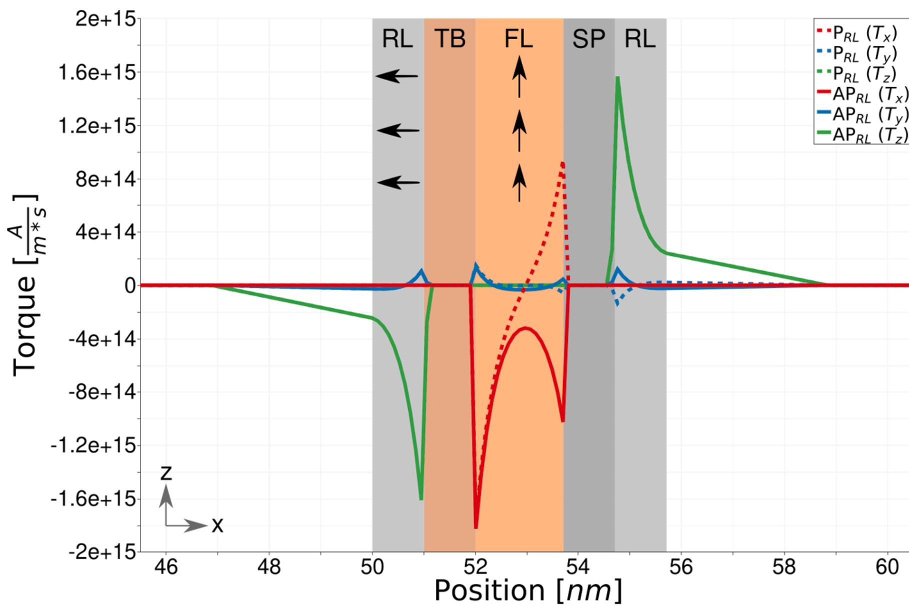

Fig. 6. Average torque on the DS-MTJ structure along the x-axis for parallel and anti-parallel RL configurations. The magnetization of the first RL points in $-\hat{x}$ and FL points in $\hat{z}$.

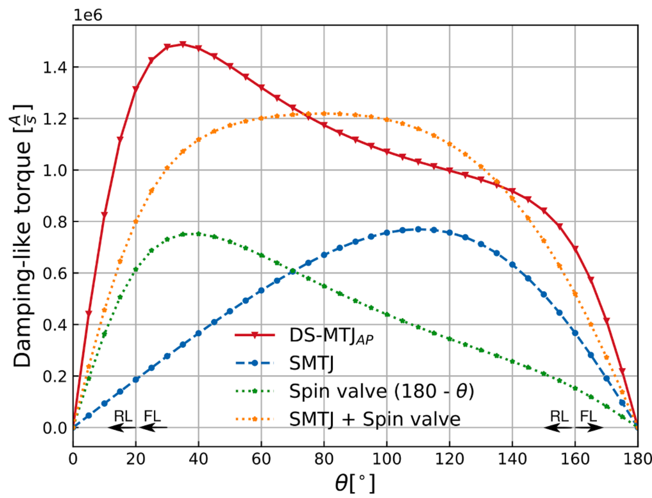

Fig. 7. Torque dependence on the magnetization angle around the y-axis for SMTJ, DS-MTJ$_{AP}$, and spin valve.

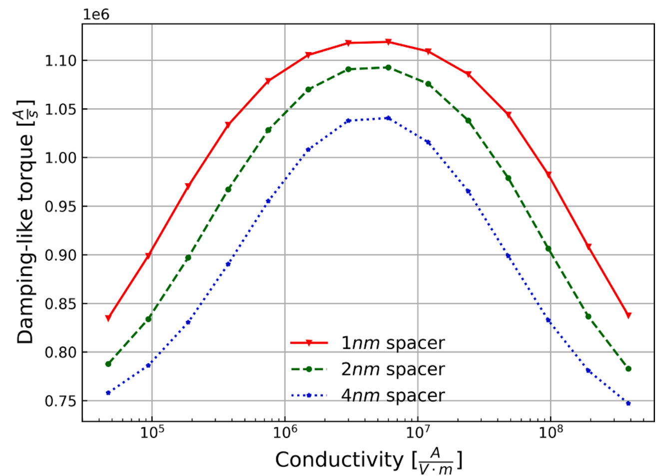

Fig. 8. Torque acting on FL in the DS-MTJ$_{AP}$ structure for different spacer conductivity σ values. The diffusion coefficient in the spacer D_e is scaled proportional to σ while λ_{sf} was unchanged. Other parameters from Table 1 including the conductivity in the metal contacts were unchanged. Maximum torque appears for the spacer conductivity value equal to that of the contacts.

structure is about 2.23 times, when switching from parallel to anti-parallel, and 2.1 times, when switching in the opposite direction.

When analyzing Figs. 2 and 3 on similar switching times, the required voltages for the DS-MTJ$_{AP}$ are about 2 times lower than the voltages for the SMTJ, in accordance with the experimental results [2].

2.2. Comparison of the structures torques

Fig. 5 shows the average components of the torque acting in the SMTJ along the x-axis. The current flows in the $-\hat{x}$ direction while the FL magnetization points in $\hat{z}$. For this structure there is a noticeable spike in the x-component close to the interface between the FL and TB, which relates to the transfer of transverse spin angular momentum. In this case, the damping-like component of the torque is uniquely defined by the general torque x-component as the magnetization of the FL points parallel to $\hat{z}$ and the one of the RL points in $-\hat{x}$.

For the DS-MTJ, the average components of the torque are shown in Fig. 6 with the same magnetization configuration and current direction as for the SMTJ. The DS-MTJ$_{AP}$ and DS-MTJ$_P$ configurations are displayed as solid and dashed lines, respectively. For the left half of the structure the torques are similar to the ones encountered in the SMTJ, however, the additional layers create further contributions whose effect on the FL depend on the relative orientation of the RLs. If the second reference layer magnetization is set anti-parallel to the original one, the torques coming from both have the same direction and thus add up, increasing the forces driving the magnetization switch. If the second RL magnetization is set parallel to that of the original one, the torques coming from both point in different directions and detract from each other, reducing the forces driving the magnetization switch. These plots directly confirm the assumption, previously based on the structure's current ratios for different RL orientations [2], that both FL interfaces receive torque contributions. This in turn, explains the reduced required voltages and switching times of the DS-MTJ$_{AP}$ in relation to the SMTJ.

Our analysis addresses the effect of torque magnitudes acting on the structures only for a fixed state of the FL magnetization. In order to have a more comprehensive view, we show in Fig. 7 the damping-like torque angular dependence, when the FL magnetization rotates on the zx-plane (starting in $-\hat{x}$ with a non-negative z-component) and the current flows along $-\hat{x}$ for the SMTJ, the DS-MTJ$_{AP}$ and the spin valve. The latter structure has the same layer stack as the SMTJ, however, instead of the tunnel barrier it employs a non-magnetic metallic spacer [1]. The addition of this structure to the comparison allows an individualized analysis of the torque contributions present in both TB|FL and SP|RL interfaces. From these results, the damping-like torque can be seen to be larger for the DS-MTJ$_{AP}$ in relation to the SMTJ for all angles, confirming that the general scenario of the damping-like torque being larger in the DS-MTJ than in a SMTJ, portrayed in Figs. 5 and 6, holds in all switching stages. The same improvement is also true for the relation between the DS-MTJ$_{AP}$ and the spin valve alone.

The sum of damping-like torque across all angles for the DS-MTJ$_{AP}$ has a value of about $3.672{\cdot}10^7 A/s$, which represents a 2.12 times increase over the SMTJ value of around $1.54{\cdot}10^7 A/s$. This shows that the 2 times reduction of required switching voltage of the DS-MTJ$_{AP}$ over the SMTJ is correspondingly accompanied by a very similar increase in the damping-like torque acting on the FL.

If the DS-MTJ is treated as the combination of a spin valve and a SMTJ then, the torque acting on the FL of the DS-MTJ in Fig. 7 can roughly be explained by the sum of the torque contributions coming from the SMTJ and the spin valve. Fig. 7 shows that there is a resemblance between the DS-MTJ and the spin valve torques, as the maximum position on the DS-MTJ curve coincides with the maximum of the curve corresponding to the spin valve. Obviously, there are more complex interactions between the layers, which help shaping the presented curve and which are not accounted for, when adding individual contributions from the structures. This explains the difference between the summed curve of the spin valve and the SMTJ in relation to the DS-MTJ.

2.3. Torque dependence on parameters

In order to asses the dependence of the torque coming from the additional RL on the spacer characteristics, we have investigated how different material-related properties affect its contributions. For all previous simulations with the DS-MTJ the conductivity of the spacer layer was set to be $\sigma = 6{\cdot}10^6$A/(V·m), as defined in [4] for a non-magnetic metallic layer. In Fig. 8 we explore the conductivity values up to two orders of magnitude lower and higher than the previously defined value. The diffusion coefficient in the spacer was also scaled proportionally while λ_{sf} was fixed. The spacer thickness was varied from 1nm to 4nm and both parameters were varied with successive multiplications by 2. The magnetization and current configurations were set as for Figs. 5 and 6.

Increasing the thickness of the spacer from 1nm to 4nm reduces the total torque for all conductivity values. Interestingly, either reducing or increasing the conductivity of the spacer with respect to the conductivity of the contacts leads the damping-like component of the torque to decrease for all spacer thicknesses. For the investigated range and

parameters the optimal torque value appears, when the spacer conductivity lies somewhere close to the conductivity value in the contacts.

3. Conclusion

We have presented the successful simulation of a novel DS-MTJ structure and its expected switching characteristics. An extensive analysis of the torque was also presented, describing the distribution of the components along the layers and their dependence on the angle of the free layer magnetization. Finally, different spacer conductivities and thicknesses were investigated. The optimal conductivity value for damping-like torque magnitude maximization along the tested range lies close to the one previously assumed in the literature, while thinner spacers give higher torques. Overall, the results from all simulations agree well with the expected behavior outlined by experimental data.

Declaration of Competing Interest

The authors declare that they have no known competing financial interests or personal relationships that could have appeared to influence the work reported in this paper.

Acknowledgments

The authors would like to acknowledge the financial support from the Austrian Federal Ministry for Digital and Economic Affairs, the National Foundation for Research, Technology and Development, and the Christian Doppler Research Association.

References

[1] Bhatti S, Sbiaa R, Hirohata A, Ohno H, Fukami S, Piramanayagam SN. Spintronics based random access memory: a review. Materials Today 2017;20(9):530–48. https://doi.org/10.1016/j.mattod.2017.07.007.

[2] Hu G, Lauer G, Sun JZ, Hashemi P, Safranski C, Brown SL, et al. 2x reduction of stt-mram switching current using double spin-torque magnetic tunnel junction. 67th Annual IEEE International Electron Devicess Meeting (IEDM) 2021:43–6.

[3] Fiorentini S, Ender J, Selberherr S, de Orio R, Goes W, Sverdlov V. Coupled spin and charge drift-diffusion approach applied to magnetic tunnel junctions. Solid-State Electronics 2021;186:108103. https://doi.org/10.1016/j.sse.2021.108103.

[4] Abert C, Ruggeri M, Bruckner F, Vogler C, Manchon A, Praetorius D, et al. A self-consistent spin-diffusion model for micromagnetics. Scientific Reports 2016;6(1): 1–7. https://doi.org/10.1038/s41598-016-0019-y.

Wilton Jaciel Loch was born in 1998 in Presidente Getúlio, Brazil. He received his Bachelor degree in Computer Science from Santa Catarina State University in 2019. In 2020 he enrolled in the Master's program in Applied Computing from the same university, with research focused on communication algorithms for high performance computing (HPC). He received his Master's degree in 2021 and in October he joined the Institute for Microelectronics to perform research on HPC methods for micromagnetic simulations of non-volatile magnetic memory devices.